

DOI: 10.1002/ijch.202100118

Review

Received: 21. October. 2021

Accepted: 18. December. 2021

Revised: 18. Dezember 2021

## Graphene Acid: a Versatile 2D Platform for Catalysis

Matías Blanco,<sup>[a]</sup> Stefano Agnoli<sup>[a]</sup>0000-0001-5204-5460,<sup>[b]</sup> Gaetano Granozzi<sup>[b]</sup>0000-0002-9509-6142\*<sup>[b]</sup>

[a] <orgDiv/>Organic Chemistry Department, <orgName/>Universidad Autónoma de Madrid.

<street/>C/ Francisco Tomás y Valiente 7, <postCode/>28049, <city/>Madrid, <country/>Spain

[b] <orgDiv/>Department of Chemical Sciences, <orgName/>University of Padova

<street/>Via Marzolo 1, I- <postCode/>35131 <city/>Padova (<country/>Italy)

phone: +39-3347151920

E-mail: Gaetano.granozzi@unipd.it

Graphene Acid

Hybrid catalysts

Heterogenization of molecular catalyst

Carbocatalysis

Electrocatalysis

Graphene acid (GA) is a novel graphene platform where the carboxylic acid groups are located in the basal plane of the carbon network. The chemical route to develop such a platform has been proposed and the final product displays a series of advantages with respect to the well-known and much used graphene oxide (GO), *i.e.* a more uniform functionalization of the graphene basal plane and an enhanced electronic conduction when compared to GO. In this review we discuss the most recent literature data which demonstrate that the excellent GA properties may have an impact on the catalytic activity of both GA itself

and the hybrid derivatives obtained using GA as a scaffold. Examples are discussed where GA as carbocatalyst, molecular catalysts heterogenized on GA and particles/GA assemblies are used as catalysts and electrocatalysts, pinpointing the advantages of using GA with respect to other graphenic substrates.

## 1. Introduction

The name “graphene” has been first proposed in 1986 by Boehm and coworkers,<sup>[1]</sup> even though within the Surface Science community the monolayer graphite was well known from the second half of the last century. Nonetheless, the real boom of graphene and other 2D materials dates back to 2004 when Geim and Novoselov proposed a simple mechanical exfoliation route to isolate and manipulate single layers.<sup>[2]</sup> This milestone demonstrated the stability of 2D materials beyond the bulk and, at the same time, that new and interesting properties arise when the lateral dimensions are constrained to the nanoscale. Then, it immediately started an impetuous race towards the exploration of the so-called materials *flatland* and of the exotic properties of this *wondermaterial*. During this first pioneering period, physicists took the lead and, besides to the description of its properties, the preparation of defect-free graphene and its scaled-up production were the most important issues that occupied the scientific efforts. Thereafter, the scientists’ focus shifted towards the so called *second generation graphenes* (SGGs) (see Scheme<sup>1</sup>),<sup>[3]</sup> that are more realistic and complex materials, including chemically modified graphene, 3D graphene architectures based on the assembly of graphene sheets and nanohybrid composites systems. This meant getting out from the strict *flatland*, and to search for possible applications of defective *real* materials endowed with a high surface specific area in a stable way (i.e. avoiding the really disappointing phenomenon of the restacking of the 2D layers). Thence, chemists started to contribute to this second race on behalf of their ability to manage complexity and diversity, so opening the route towards the very challenging and strategic topics of catalysis, energy conversion and storage, sensors and environment remediation.

A prototypical material that boosted this second race was graphene oxide (GO) (see Figure 1a). With respect to graphene, it is an *ill-defined* material where several functional groups (carboxylic acid, hydroxylic groups, ketones, lactones, etc.) occupy random positions and the extended defectivity is hard to be uniquely described.<sup>[4]</sup> In order to break the Van der Waals interactions between the single graphene layers in pristine graphite, aggressive oxidation methods (e.g. Hummers oxidation, Brodie oxidation and their modifications, for instance) must be carried out to increase the interlayer distance from typically 0.34 nm to more than 1.0 nm.<sup>[5a]</sup> However, this has also the effect of disrupting the C-C sp<sup>2</sup> scaffold and introducing oxygen containing functional groups. The oxidation generates a material called graphite oxide that possesses a C/O atomic ratio below 1 with an electrical insulating character and high dispersability in polar solvents such as water. Graphite oxide can be easily exfoliated by ultrasonication treatments to yield few layers 2D GO nanosheets, which typically keep maintain graphite oxide properties.<sup>[5]</sup>

It is easy to conceive that the general structure of GO is chaotic as a result of this non-reproducible and very aggressive preparation procedure.<sup>[6a]</sup> The lateral dimension of GO varies from few nm (the so-called graphene quantum dot) to several μm or even mm. In addition, the persisting aromatic domains (typically, the C sp<sup>2</sup> content of GO is less than 40%) are randomly distributed within the sheet, thus imparting an insulator character to GO, which however can be transformed into a conductive material by thermal or chemical reduction (forming reduced-GO, rGO).<sup>[6]</sup>

Moreover, the degree of exfoliation varies from the single to few layers (i.e. less than 10 vertically stacked graphene sheets) as a function of the applied ultrasonication protocol. Furthermore, general consensus describes the surface oxygen chemistry in a way where sterically impeded moieties, such as the COOH groups, are located at the edges of the nanosheet

or at the defects within the basal plane, while less reactive functionalities (hydroxylic and epoxy groups) are mainly located at the basal plane.<sup>[7]</sup>

Usually, GO is easily dispersed in polar solvents, it can be produced at high yield with relative slight efforts and it is quite reactive, which makes this material a convenient stepping stone for the development of SGGs. Indeed, the literature reports ~~numerous works~~ several papers that aim to make GO the flagship in the development of graphene hybrid nanomaterials. Its rich surface chemistry allows GO to react with a wide gamut of reagents,<sup>[7c]</sup> and therefore it offers the possibility to immobilize nanoparticles and molecular catalysts, which is the target for the preparation of hybrid materials that are often applied as catalysts or sensors.<sup>[8]</sup> Nevertheless, the chemical versatility of GO is at the expenses of precise chemical control, therefore GO can be hardly used as a *model* system where investigate the effects of a graphene heterogenized with a specific functional moiety.<sup>[8d]</sup> This calls for the development of alternative materials where study, in a more rigorous manner, the effects of the graphene functionalization, so that clear structure-functionality relationships could be established.

In the last few years a new entry in the list of potentially useful building blocks to prepare SGGs has been introduced: it has been named graphene acid (GA) and its peculiarity is the presence of carboxylic acid groups directly attached to the carbon  $sp^2$  skeleton. In fact, the COOH groups allow an easy and uniform functionalization of the graphene basal plane by exploiting their rich and selective chemistry, with the benefit of avoiding possible side reactions due to lack of other oxygen based functional groups, which on the other hand are typical of standard GO.

However, it has to be outlined that the term GA has been assigned to very different COOH-rich systems. Some authors called GA a material prepared starting from GO by subsequent strong oxidation steps.<sup>[9]</sup> In this case, a concentration of about 30<sup>wt%</sup> of COOH can be obtained, but the final product loses the typical platelet structure of GO, and a 3D pattern

is reached showing aggregates of particles with a size of hundreds of nm. Furthermore, a wrinkled 3D structure, originated from strong interactions of the individual small GA sheets through hydrogen bonds, is typically observed.<sup>[9]</sup> High resolution photoemission spectra showed that on passing from GO to this GA, the C/O ratio decreases from 1.95 to 1.28 and the photoemission peak related to C sp<sup>2</sup> disappears, achieving an overall stoichiometry estimated to be C<sub>1</sub>(COOH)<sub>1</sub>. So, the final GA obtained by this procedure is very far from a simply graphene sheet substituted in the basal plane.

On the other hand, following a completely different route starting from fluorographene and passing through the cyanographene intermediate (see Section<sup>^2</sup>), other authors have reached a completely different material, denoted again as GA.<sup>[10]</sup> In this case, a platelet like morphology is maintained as well as the presence of a large fraction of graphitic sp<sup>2</sup> carbon. However, the basal plane is densely (upto 10<sup>^at.%</sup>) and homogenously functionalized with -COOH groups with an estimated stoichiometry of C<sub>6,6</sub>(COOH)<sub>1</sub> (see Figure<sup>^1<xfigr1>b</sup>).<sup>[10]</sup> The strong points of this new material are an excellent electronic conductivity, biocompatibility, dispersibility in water and a higher homogeneity of the oxygen surface groups with respect to GO. This last point in particular, makes GA an attractive materials platform for chemical functionalization.

In the present minireview, we will focus on the second type of GA, i.e. the one presenting the carboxylic groups on the basal plane. In section 2, we will give an account of its preparation and structure, based on several characterization studies. Thereafter, in Section<sup>^3</sup> we will describe the so far reported studies where the peculiar properties of GA are exploited in different applications.

## 2. Preparation and Characterization of Graphene Acid

In 2017, Bakandritsos *et al.* firstly reported the preparation of GA according to the route schematized in Figure<sup>^2<figr2></sup>, which starts from a stable, stoichiometric and well-

defined graphene derivative, i.e. fluorographene (FG).<sup>[10a]</sup> The first step toward the synthesis of GA consists in transforming FG into fluorine-free cyanographene, which is then hydrolyzed in acid conditions to GA. More in detail, commercial fluorographite is suspended in dimethylformamide (DMF) and sonicated under nitrogen atmosphere for several hours, then providing few layer FG, and thereafter a cyanide source, typically KCN, is added to the suspension and let to react at 130°C for 24 h, to promote the nucleophilic substitution of fluorine ions with the cyanide ions, taking advantage of the peculiar properties of FG where the F-C-C bond is labile.<sup>[10b]</sup>

The suspension is then diluted in acetone and washed by centrifugation with fresh and hot (80°C) DMF, dichloromethane, acetone, ethanol, and water for 3 times. In the second step, the newly installed cyano groups are hydrolyzed in 20% HNO<sub>3</sub> under reflux at 100°C for 24 h, to convert the CN groups into the COOH groups. Finally, the material is washed again by following the same centrifugation protocol described above.

Through the above mentioned procedure, it was possible to prepare GA nanosheets with a functionalization degree with COOH groups of about 13%, whereas less than 1% of F atoms are left. Notably, micro-Raman spectroscopy experiments demonstrated the intensity ratio between the D and G band remains almost the same both on edges (1.09) and basal plan (1.15), suggesting a very homogeneous functionalization. This is a notable difference with GO, where the carboxyl groups are selectively observed at the edges of the graphene sheets.

Another key difference with GO is the extremely good conductivity of GA. Direct electrical measurements by four probe method indicated that the sheet resistance is  $6800 \Omega \text{sq}^{-1}$ , which is a value several orders of magnitude higher than GO. The enhanced electronic conduction of GA compared to its FG precursor and GO is also confirmed by electrochemical measurements: GA based electrodes are very stable, have excellent electron transfer properties (charge transfer resistance of about 80 Ω), typical of reversible

electrodes, can sustain large currents in a wide electrochemical potential and show limited capacitance.<sup>[10a,11]</sup>

The explanation for these notable electrical properties, that are quite unique among functionalized graphenes, have been rationalized by Density Functional Theory (DFT) calculations.<sup>[10a]</sup> The presence of carboxyl groups opens indeed a small gap in graphene band structure but it introduces also a large number of intragap states. The details of the electronic structure notably depend on the amount of carboxyl groups and their local arrangement, however for a functionalization degree between 2.15 and 16.7%, GA shows the electronic features of a low band gap semiconductor with intragap states frequently lying very close to the Fermi level. The morphology of GA ~~derivatized-obtained by from~~ fluorinated graphite has been routinely investigated by AFM, SEM and TEM.<sup>[10]</sup> The features of the final materials (thickness, lateral extension of the nanosheets) depend on the details of the synthetic procedure (time of sonication, duration of the reaction, concentration etc.) and properties of the initial raw precursor (i.e. fluorinated graphite). Anyway, it has been widely reported the possibility to obtain a large fraction of single layers, while in general the lateral extensions of the nanosheets is not larger than a few hundred ~~ths~~ of nm, dimensions significantly smaller compared to the typical materials produced by graphite oxidation.

### 3. The Uses of Graphene Acid

As depicted in the previous section, GA is a very appealing nanosized platform for the facile preparation of SGGs. The main advantages of GA with respect to GO are: i) good electron conductivity ii) preservation of aromaticity, iii) the relatively high amount of homogeneously distributed COOH groups, ~~both~~ on the basal plane, ~~and edges~~. In the following section we will briefly outline the main achievements so far reached with the use of GA.

#### 3.1 Graphene Acid Itself as a Catalyst and Electrocatalyst

The fundamental pillar of the carbocatalysis research area is the presence of oxygen surface groups and aromatic domains within the structure of a carbon material: in this case the carbon material as a whole, or some specific regions, may act as active site to speed up chemical conversion. One of the first carbocatalytic examples that employed carbon nanomaterials was reported by Bielawski and coworkers,<sup>[12]</sup> who demonstrated that GO was able to convert alcohols, alkenes, and alkynes to aldehydes or ketones with an easy and cheap process. Nevertheless, an issue has been risen in literature because the authors needed to employ a neat reaction at 150 °C using a loading of 400% of GO vs substrate to reach such targets. Thence GO in this case can be hardly defined as a catalyst, but rather as a stoichiometric reagent.<sup>[13]</sup> It has also to be mentioned that the chemical activity of GO was recently challenged, and proposed that the metal contaminants present in the materials are indeed the true active species and not the carbon.<sup>[14]</sup>

In a recent paper by our group we demonstrated that the situation is much different when GA is used in presence of HNO<sub>3</sub> as a co-catalyst.<sup>[15]</sup> In this case benzyl alcohol was fully oxidized in just 2 h at 90 °C with a catalyst loading of 5% wt. of GA using just catalytic amounts of HNO<sub>3</sub> (Figure 3a). This activity set a new benchmark in carbocatalysis: 152 mmol of substrate were converted per gram of catalyst and per hour, which is a better performance compared to other carbocatalysts and even previously reported noble metallic systems.<sup>[12c,15b-d]</sup> Notably, under the same experimental conditions, GO showed negligible activity. In addition, GA could be recycled for more than 10 reaction runs without any appreciable modification of its structure or surface chemistry. To be sure that the catalytic activity was indeed related to GA, it was carefully checked and then excluded the possible presence of metal impurities, confirming that the GA is indeed a metal free carbocatalyst. The well-defined surface chemistry of GA allowed us to conceive a reductionistic experimental plan and to model accurately the reaction by DFT calculations, leading us to propose the catalytic cycle reported in Figure 3b. The improved performance of GA was related



to the peculiar structure of the material and the synergistic effects with the co-catalyst during the catalytic cycle. Thus, the use of  $\text{HNO}_3$  was not futile, since the calculations demonstrated that the COOH groups were able to selectively bind  $\text{HNO}_3$  to promote a GA-mediated electron transfer that yields  $\text{NO}_2$ , which was also observed experimentally:  $\text{NO}_2$  was not stable in the reaction medium and generated  $\text{HNO}_2$ , which was able to undergo a condensation to yield an organic nitrite (also detected in the experiments), which is finally oxidized at the surface of the GA to yield the final product. Hence, several redox reactions take place during this catalytic cycle; therefore, the possibility of GA to store and transfer on demand electrons giving its conductive nature combined with the high density of COOH groups are key to catalyse the oxidation. On the other hand, these synergic effects are not possible on GO whose carboxyl groups are electrically disconnected from the rest of the carbon material, which, combined with its defectivity, hinders the electrons storing and supply needed in the redox cycle.

Very recently, Sanad and coworkers took advantage of the catalytic potential and good electron conduction of GA to develop an electrocatalyst able to carry out the non-enzymatic glucose oxidation reaction and the oxygen reduction reaction (ORR), achieving improved performance compared to rGO.<sup>[16]</sup> These authors concluded that the increased number of COOH groups on GA compared to rGO resulted in a significantly higher ORR activity with an onset potential of 0.8 V, the highest reported for graphenic materials. In addition, they related the improved glucose oxidation kinetics to the large number of electron-withdrawing COOH moieties on the basal plane of GA, combined with the larger intrinsic conductivity. In another work, Zhang *et al.* tested N-GA (N-doped GA) as an efficient electrocatalyst for the  $\text{H}_2\text{O}_2$  production.<sup>[17]</sup> This particular material selectively catalyses the oxygen reduction reaction (ORR) through the two electron pathway, with a faradaic efficiency which reaches a maximum value of 70% in acidic media (pH= 0.96). In addition, it achieves also a remarkable  $\text{H}_2\text{O}_2$  productivity in long term bulk electrolysis, which, under optimized conditions, could

accomplish the outstanding value of  $107.8 \text{ mmol} \cdot \text{g}^{-1} \cdot \text{h}^{-1}$ , outperforming a commercial GO benchmark both in terms of activity and selectivity (Figure 4a).

Extended XPS analysis, control experiments (using decarboxylated N-GA heated at high temperature) and DFT calculations confirmed that the surface COOH groups play a significant role in achieving the high activity (7-fold higher than non-carboxylated samples) and accelerating the reaction. In particular, the DFT calculations demonstrated that the surface COOH groups in N-GA participate to the  $\text{H}_2\text{O}_2$  formation by favouring a rapid surface  $\cdot\text{OOH}$  radical formation through a spontaneous hydrogen transfer reduction (Figure 4b).

### 3.2 Heterogenization of Molecular Catalysts on Graphene Acid

In the previous section we described the use of GA as a catalyst, but GA can contribute to catalysis also through another way. In fact, the peculiar surface chemistry of this special material, given the high homogeneity of its COOH surface groups, is very appealing for the immobilization of a molecular catalyst. The heterogenization of molecular catalysts has recently attracted a lot of attention because it might combine the advantages of both heterogeneous and homogeneous catalysts, i.e. the high activity and selectivity of the latter, with the stability over time, recyclability, and up-scaling of the former.<sup>[18]</sup> Thence, hybrid catalytic systems where efficient molecular catalysts are immobilized on a suitable substrate can really play an important role in expanding the impact of catalysis.

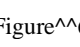

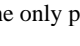
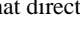
In the specific case of hybrid catalysts engineered on GA, the actual merits of GA can be clearly recognized when the properties of the GA-based hybrid material, in regards to both the functionalization protocol and the catalytic activity, are compared with those of analogous GO hybrids. Two different strategies have been reported for the efficient immobilization of a molecular catalyst at GA surface. The first is based on the covalent binding through amide bonds using the COOH surface groups of GA, typically employing the coupling agents to selectively generate the intended amide-type bond without interacting with other chemical

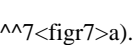
groups.<sup>[18]</sup> The second strategy is based on non-covalent interactions, generally electrostatic interactions, between the COOH groups of GA and a possible modifier.

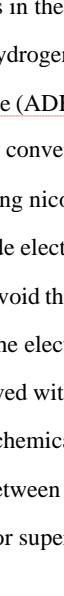
### 3.2.1 Covalent Functionalization

Regarding the covalent approach, in a recent paper we were able to demonstrate the immobilization of ferrocene (Fc) moieties through covalent bonds on the surface of GA.<sup>[11]</sup> Figure<sup>5</sup>a shows the two-step synthesis route: in the first step, free-amino groups pendants endings were produced by reacting GA with 1,3-diaminopropane (PDA), which in the second step were reacted with ferrocenecarboxylic acid. For benchmarking purposes, the same functionalization protocol was applied to GO. Indeed, a different functionalization degree was clearly observed between the two materials: according to XPS characterizations, GA was able to covalently bind 3.6% at. of iron as Fe<sup>2+</sup>, while GO only reached 1.0% at. of iron, and more important, 40% of this metal was Fe<sup>3+</sup> (Figure<sup>5</sup>b). Hence, the controlled surface chemistry of GA promotes efficiently the immobilization of the molecular catalyst without inducing any modification. Both GA-PDA-Fc and GO-PDA-Fc hybrid materials were tested as catalysts for the C-H insertion of diazonium salts on arene substrates, a reaction that is easily catalyzed by molecular Fc. Interestingly, the GA-PDA-Fc hybrid revealed an enhanced activity when compared both to the homogeneous Fc and the heterogenized GO-PDA-Fc catalysts in the aforementioned insertion reaction (Figure<sup>5</sup>c). This advantage of using GA-PDA-Fc is even more marked when employing as reaction substrate higher condensed polyaromatics (Figure<sup>5</sup>c inset). Indeed, GA-PDA-Fc hybrid reached 60% conversion of the phenyl-naphtyl insertion product in 24 h of reaction, while GO analogous material saturated at 47% conversion after 50 h. The best result was obtained using anthracene as substrate (>99% conversion). We suggested to relate the enhanced activity of GA-PDA-Fc to the presence of aromatic domains close to the catalytic active sites: the large sp<sup>2</sup> patches present in GA amid the


COOH groups allow an efficient  $\pi$  stacking of the substrate close to the bonded Fc ring. As a result, the kinetics of the reaction is facilitated. Furthermore, the conductivity of GA assists in the redox reactions that sustain the catalytic cycle. Conversely, such phenomena cannot take place neither in the homogeneous phase nor in GO-PDA-C-Fc sample due to the highly insulating character of the GO moiety.

Another example of covalent functionalization of GA has been recently reported:<sup>[19]</sup> we were able to graft at the GA surface, again through the carbodiimide chemistry, a Co-based molecular catalyst very active for artificial photosynthesis, namely cobalt quaterpyridine (Coqpy). In this case, the Coqpy complex was modified to bear a free NH<sub>2</sub> group (Figure<sup>6</sup>) which was directly attached to the COOH groups, achieving a 4.6% wt. loading of Co. The hybrid material was thoroughly characterized by XPS, X-ray absorption spectroscopy (both XANES and EXAFS spectra), IR and Raman spectroscopies and high-resolution transmission electron microscopy (HR-TEM). The interesting point is that GA can directly interact with the metallic center since COOH groups adjacent to the grafting site enter into Co coordination sphere (Figure<sup>6</sup>) through the loss of the chlorine ligand of the free complex, as schematized in Figure<sup>6</sup>. This quite peculiar structure proved to be highly active in the visible-light driven CO<sub>2</sub> catalytic conversion in acetonitrile solutions with complete selectivity control (Figure<sup>6</sup>). Indeed, the product distribution could be completely switched upon adjusting the experimental conditions. Thus, production of CO as the only product was achieved when using a weak acid (phenol or trifluoroethanol) as a co-substrate. On the other hand, formate was exclusively obtained in mild basic solutions of mixed acetonitrile and triethanolamine. Moreover, exceptional stabilities for over 200 h of irradiation were obtained without compromising the selective conversion of CO<sub>2</sub> to products (>97%) in both different setups. The interactions between the metal and the material through that direct bonding were concluded to be responsible for this excellent behaviour.

GA is also an emerging material with a still an untapped potential in the field of biocatalysis. Using a different coupling agent, Seelajaroen and coworkers grafted a dehydrogenase (DH) enzyme on the carboxylic acids of GA (G-DH).[20] In this particular example, the carboxylic acids of the material were covalently modified with a sulfo-succinimide that subsequently reacted with an amino- terminated aminoacid of the DH (Figure<sup>7</sup>.

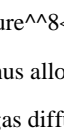
Logically, the amount of enzyme bonded was very low compared to other molecular catalysts as a result of steric hindrance effects (or maybe changes in the spatial conformation of the protein). Three DH enzymes were tested, i.e. formate dehydrogenase (F<sub>ate</sub>DH), formaldehyde dehydrogenase (F<sub>ald</sub>DH) and alcohol dehydrogenase (ADH), yielding three different hybrid enzymes. respectively, which were tested for the conversion of CO<sub>2</sub> to methanol by two different approaches: (i) chemical reduction using nicotinamide adenine dinucleotide (NADH) as cofactor and (ii) the NADH-free cascade electroreduction (Figure<sup>7</sup>). In the second case, authors succeeded to avoid the use of NADH as sacrificial cofactor owing to the efficient electron transfer from the electrode onto the nanobiohybrid catalyst. A faradaic efficiency of 12% was achieved with high selectivity and low overpotential (0.61 V) considering the six-electron electrochemical reduction performed. The authors concluded that the covalent interaction between the enzyme and GA are responsible of the reported milestones, being also comparable or superior to other state-of-the-art electrocatalysts.

### 3.3.2 Non Covalent Functionalization

Recently, Reuillard *et al.* described the use of GA nanosheets to obtain new electrode materials for the reversible electrocatalytic hydrogen oxidation reaction (HOR) exploiting noncovalent electrostatic interactions to graft a NiArg bioinspired electrocatalyst on GA (see Figure<sup>8</sup>).<sup>[21]</sup> The highly functionalized and conductive GA provided a large

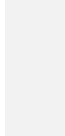
ha formattato: Pedice

ha formattato: Pedice

amount of electrostatically anchoring sites for the catalyst (Figure<sup>8</sup>) while ensuring excellent electronic wiring of the molecular catalyst, thus allowing the development of an efficient molecular-based anode for HOR developed on a gas diffusion layer (GDL) to be used in fuel cells. The NiArg complex bears four arginine moieties (and therefore four guanidine fragments), which allow it to electrostatically interact with the carboxylic acids of GA. With this very simple immobilization strategy, the optimized electrode-catalyst assembly has reached new benchmark electrocatalytic performances for heterogeneous molecular HOR, with current densities above  $30 \text{ mA cm}^{-2}$  at  $0.4 \text{ V}$  versus reversible hydrogen electrode in acidic aqueous conditions and at room temperature.

Control experiments demonstrated that the level of activity reached was only caused by the interactions between the Ni complex and the material. Indeed, neither the homogeneous test nor Ni nanoparticles deposited on GA achieved those record results.

### 3.4 Nanoparticles and Single Metal Atoms Immobilization on Graphene Acid

The two previous sections dealt with the intrinsic catalytic properties of GA or with heterogenized molecular catalysts easily grafted on it due to its well-defined surface chemistry. But the *new chemistry* is not limited to these points. The high electronic mobility at the basal plane of the material altogether with the presence of highly reactive sites make GA also an ideal platform to immobilize nanoparticles, again for catalysis purposes.<sup>[22]</sup> For instance, we have reported on the growth of palladium nanoparticles on GA, obtained by mixing palladium acetate with GA in different proportions according to the route reported in Figure<sup>9</sup>a. We envisioned that the large number of COOH would have been able to sustain counterion metathesis reactions in order to fix Pd ions on the surface. After electron transfer from GA, a seed is generated that serves for a nucleation site for the eventual metallic nanoparticle growth. Actually, we found that the size of the final nanoparticles is related to the amount of metal precursor added: from sharp distribution of  $0.6\text{--}0.8 \text{ nm}$  clusters using  $0.25$

equivalents of Pd(OAc)<sub>2</sub> (GA<C->Pd-25) to 3--4<sup>nm</sup> nanoparticles using 1 equivalent of Pd(OAc)<sub>2</sub> (GA<C->Pd-100) (see Figure<sup>9</sup><figr9>b). The presence of the COOH reduces the mobility of the metallic nanostructures, so avoiding the Ostwald ripening and driving an exquisite size distribution control during their growth. Conversely, a benchmark GO achieved broad distributions of nanoparticles with sizes ranging 18--40<sup>nm</sup>.

The insulating nature of GO due to the misconnection between the aromatic domains and the heterogeneous oxygenchemistry distribution were concluded to lead to a less effective synthesis. Very interestingly, this hybrid material is very active for the Suzuki–Miyaura (SM) cross coupling reaction of boronic acids and organic halides (see Figure<sup>10</sup><figr10>a) with high yields and selectivity under environmentally- friendly conditions, reaching a performance comparable to the state-of-the-art catalysts. In particular, GA<C->Pd-25 resulted the most active material, reaching a conversion above 99% after only 2<sup>min</sup> of thermal equilibration, with a turnover frequency (TOF) of 30030<sup>h<sup>-1</sup></sup>, while GA<C->Pd-100 completed the reaction in 60<sup>min</sup>.

In Figure<sup>10</sup><figr10>b we compare the kinetic profiles of the SM reaction using either the GA<C->Pd or GO<C->Pd catalysts: notably, the performance is superior to that of the benchmark GO<C->Pd-100, which showed 98% conversion with poorer activity, and also superior to that of homogeneous Pd(OAc)<sub>2</sub>. In addition, all sample presented activity for the homocoupling of boronic acids, therefore representing a very versatile catalyst able to perform different reaction pathways as a function of the conditions. But more important to say is the greener performance of the material. While all the SM reactions were performed in water and aerobic conditions, almost negligible Pd leaching was detected during and after reactions. Indeed, ppb levels of Pd were determined by ICP analysis in the reaction waters, while hot filtration experiments confirmed the absence of active species in solution.

Interestingly, very recently the anchoring of single-atom transition metals to GA for catalysis purposes has been also investigated theoretically.<sup>[23]</sup> they calculated the bond dissociation energy and charge exchange, solvent effects on the coordination of the metal (Fe, Co, Ni, Ru, Rh, Pd, Cu, Ag, and Au in different oxidation states) to GA and the XPS binding energy of the hypothetical hybrids for their easy identification. Authors considered the calculated samples stable enough to be considered suitable single atom catalysis, although they admitted that some competitive phenomena could experimentally occur. They concluded that the GA<C->M bond strength is to be related to the amount of charge transfer between the metal and substrate and depends on the electron affinity of ~~a~~the particular metal. They also stated that the anchoring of metal cations was generally associated with metal reduction as a function of HOMO-LUMO alignment between the metal and the  $\pi$  system of the material.

Sanad and coworkers deposited Sm<sub>2</sub>O<sub>3</sub> particles (see Figure<sup>11</sup><figr1>a) on GA, and explored its electrocatalytic performance for glucose oxidation (Figure<sup>11</sup><xfigr1>b) and ORR compared to an analogous Sm<sub>2</sub>O<sub>3</sub>/rGO sample.<sup>[16]</sup> Sm<sub>2</sub>O<sub>3</sub>/GA presented a good electrocatalytic behaviour developing a glucose oxidation current of 0.62 mA and an ORR activity with an onset potential of 0.8 V and a half-wave potential of 0.75 V vs RHE. From the comparison between Sm<sub>2</sub>O<sub>3</sub>/rGO and Sm<sub>2</sub>O<sub>3</sub>/GA the authors concluded that the faster electron transfer in the latter is attributable to the already mentioned higher electronic conductivity of GA. In addition, these authors elucidated the active sites for the glucose oxidation activity by a combination of experiments and calculations (Figure<sup>11</sup><xfigr1>c), and concluded that the Sm<sub>2</sub>O<sub>3</sub>/GA has a lower charge-transfer resistance, better HOMO-LUMO alignment, reduced charge-transfer resistance and substrate (glucose or oxygen) binding affinity, ~~resulting in a further enhanced~~. In the same paper the authors explored the use of the Sm<sub>2</sub>O<sub>3</sub>/GA as a sensor of glucose in different environments.<sup>[16]</sup> Hence, the same electrode containing the Sm<sub>2</sub>O<sub>3</sub>/GA was tested in artificial and saliva samples for the detection of glucose. The sensor took advantage of the electrochemical sensibility of the



system towards the saccharide oxidation because a peak at  $\sim 0.62$  V vs RHE merged out in the voltammograms in the presence of the analyte. Thus, chronoamperometric (CA) measurements were conducted varying the glucose concentration from  $100$  nM to  $10$  mM and variations in the current were recorded (Figure 12).

The device could reach a limit of detection (LOD) of  $107$  nM and a sensitivity of  $20.8$   $\mu$ A/ $\mu$ M for glucose sensing. It is worthy to mention that GA itself could act as glucose sensor, under these experimental conditions, even though the presence of  $\text{Sm}_2\text{O}_3$  nanoparticles enhanced the sensitivity similar or superior to other state-of-the-art nonenzymatic sensors without major interferences of other biomolecules and good stability for more than 5000 electrochemical cycles.

#### 4. Conclusions and Perspectives

In the present review we have focused on the catalytic applications of a new graphene derivative, *i.e.* GA. In particular, GA has been successfully employed as an efficient carbocatalyst able to outperform state-of-the-art catalysts in the oxidation of organic alcohols, including GO and noble metal systems. In addition, the particular and unique surface chemistry of GA allows an easy and versatile functionalization. Herein we have reported different strategies adopted for the covalent immobilization for instance of iron, nickel and cobalt organometallic complexes, but also enzymes and nanoparticles. Thus, GA represents a valuable alternative to GO in many useful applications.

However, in order to be a real alternative to GO, which is the current workhorse for most practical applications of graphene, some major issues should be solved. The first one is associated with the actual preparation route of GA, which is far from being *green*, given the use of toxic substances (cyanide) and solvents with a high environmental impact (DMF). Preparation methods alternative to present one, *which are greener* and easily scalable, would represent a key step for a widespread use of GA. Among them, electrochemical oxidation does

not represent a viable option since it is very hard to achieve an oxidation level up to carboxyl acids, especially on the basal plane.<sup>[25]</sup>

Another key aspect is the control of morphology and the possibility of assembling GA sheets to produce more complex nanostructures. In the case of graphene and GO, several different morphologies of the sheets have been proposed according to the targeted applications: millimeter wide single sheets<sup>[24a]</sup> and quantum dots,<sup>[24b]</sup> nanoribbons<sup>[24c]</sup> and nanostripes,<sup>[24d]</sup> holey sheets<sup>[24e]</sup> and wrinkled sheets<sup>[24f]</sup> are only some of the many faces of SGGs. On the contrary, so far, GA has been obtained only as few layer submicrometric sheets and no attempts have been made to control more precisely its morphology. Moreover, for many applications it is important to achieve an organization beyond the single sheet as confirmed by many works dealing on the preparation of 3D nano or meso or even macro structures. Applications in catalysis, membranes, separation and purifications technologies, sensors often intrinsically require the production of 3D materials or can obtain great advantages for a 3D hierarchical organization. GA, given the presence of carboxyl groups, is poised to easy self-assembly, as also demonstrated in the very first work by Otyepka *et al.*,<sup>[10a]</sup> where center-diverging dendritic mesostructures were produced. However, so far, no further attention has been given to this topic.

In conclusion, the materials science of GA is only at the beginning and many fundamental properties have still to be fully elucidated, e.g. magnetism or interaction with light. Once more amenable methods for its synthesis will be found, we expect that GA will soon emerge from a too restricted flatland.

#### **Acknowledgements**

Financial support from the two Italian Ministers, MIUR (PRIN 2015: SMARTNESS, No. 2015^K7FZLH; PRIN2017: Multi-e, No. 20179337R7) and MAECI (Italy-China Bilateral Project, GINSENG, No. PGR00953) are gratefully acknowledged. M.B. wishes to thank the Spanish Government for a Juan de la Cierva contract (IJC2019- 042157-I).

- <lit1><jnl>H.<sup>^</sup>P. Boehm, R. Setton, E. Stump, *Carbon* **1986**, *24*, 241--245</jnl>.
- <lit2><jnl>K.<sup>^</sup>S. Novoselov, A.<sup>^</sup>K. Geim, S.<sup>^</sup>V. Morozov, D. Jiang, Y. Zhang, S.<sup>^</sup>V. Dubonos, I.<sup>^</sup>V. Grigorieva, A.<sup>^</sup>A. Firsov, *Science* **2004**, *306*, 666--669</jnl>.
- <lit3><jnl>S. Agnoli, G. Granozzi, *Surf. Sci.* **2013**, *609*, 1--5</jnl>.
- <lit4><jnl>K. Erickson, R. Erni, Z. Lee, N. Alem, W. Gannett, A. Zettl, *Adv. Mater.* **2010**, *22*, 4467--4472</jnl>.
- <lit5><lit\_a><jnl>Y. Zhu, S. Murali, W. Cai, X. Li, J.<sup>^</sup>W. Suk, J.<sup>^</sup>R. Potts, R.<sup>^</sup>S. Ruoff, *Adv. Mater.* **2010**, *22*, 3906--3924</jnl>; <lit\_b><jnl>C. Hontoria-Lucas, A.<sup>^</sup>J. López-Peinado, J. de<sup>^</sup>D.<sup>^</sup>López-González, M.<sup>^</sup>L. Rojas-Cervantes, R.<sup>^</sup>M. Martín-Aranda, *Carbon* **1995**, *33*, 1582--1592</jnl>; <lit\_c><jnl>A.<sup>^</sup>M. Dimiev, J.<sup>^</sup>M. Tour, *ACS Nano* **2014**, *8*, 3060--3068</jnl>.
- <lit6><lit\_a><jnl>K.<sup>^</sup>A. Mkhoyan, A.<sup>^</sup>W. Contryman, J. Silcox, D.<sup>^</sup>A. Stewart, G. Eda, C. Mattevi, S. Miller, M. Chhowalla, *Nano Lett.* **2009**, *9*, 1058--1063</jnl>; <lit\_b><jnl>F. Liu, M.-H. Jang, H. Dong<sup>^</sup>Ha, J.-H. Kim, Y.-H. Cho, T.<sup>^</sup>S. Seo, *Adv. Mater.* **2013**, *25*, 3657--3662</jnl>; <lit\_c><jnl>K. Krishnamoorthy, M. Veerapandian, K. Yun, S.-J. Kim, *Carbon* **2013**, *53*, 38--49</jnl>; <lit\_d><jnl>C. Mattevi, G. Eda, S. Agnoli, S. Miller, K.<sup>^</sup>A. Mkhoyan, O. Celik, D. Mastrogiovanni, G. Granozzi, E. Garfunkel, M. Chhowalla, *Adv. Funct. Mater.* **2009**, *19*, 2577--2583</jnl>.
- <lit7><lit\_a><jnl>D.<sup>^</sup>A. Dikin, S. Stankovich, E.<sup>^</sup>J. Zimney, R.<sup>^</sup>D. Piner, G.<sup>^</sup>H.<sup>^</sup>B. Dommett, G. Evmenenko, S.<sup>^</sup>T. Nguyen, R.<sup>^</sup>S. Ruoff, *Nature* **2007**, *448*, 457--460</jnl>; <lit\_b><jnl>D.<sup>^</sup>R. Dreyer, S. Park, C.<sup>^</sup>W. Bielawski, R.<sup>^</sup>S. Ruoff, *Chem. Soc. Rev.* **2010**, *39*, 228--240</jnl>.
- <lit8><lit\_a><jnl>H. Zhao, Q. Zhu, Y. Gao, P. Zhai, D. Ma, *Appl. Catal. A* **2013**, *456*, 233--239</jnl>; <lit\_b><jnl>H. Tang, H. Yin, J. Wang, N. Yang, D. Wang, Z. Tang, *Angew.*

ha formattato: Tedesco (Germania)

*Chem. Int. Ed.* **2013**, *53*, 5585--5589</jnl>; <lit\_c><jnl>L. Gao, C. Lian, Y. Zhou, L. Yan, Q. Li, C. Zhang, L. Chen, K. Chen, *Biosens. Bioelectron.* **2014**, *60*, 22--29</jnl>; <lit\_d><jnl>M. Blanco, P. Álvarez, C. Blanco, M.<sup>^</sup>V. Jiménez, J. Fernández-Tornos, J.<sup>^</sup>J. Pérez-Torrente, J. Blasco, G. Subías, V. Cuartero, L.<sup>^</sup>A. Oro, R. Menéndez, *Carbon* **2016**, *96*, 66--74</jnl>.

<lit9><jnl>O. Jankovský, M. Nováček, J. Luxa, D. Sedmidubský, V. Fila, M. Pumera, Z. Sofer, *Chem. Eur. J.* **2016**, *22*, 17416--17424</jnl>.

<lit10><lit\_a><jnl>A. Bakandritsos, M. Pykal, P. Błoński, P. Jakubec, D.<sup>^</sup>D. Chronopoulos, K. Poláková, V. Georgakilas, K. Čépe, O. Tomanec, V. Ranc, A.<sup>^</sup>B. Bourlinos, R. Zbořil, M. Otyepka, *ACS Nano* **2017**, *11*, 2982--2991</jnl>; <lit\_b><jnl>M. Medved', G. Zoppellaro, J. Ugolotti, D. Matochová, P. Lazar, T. Pospíšil, A. Bakandritsos, J. Tuček, R. Zbořil, M. Otyepka, *Nanoscale* **2018**, *10*, 4696--4707</jnl>.

<lit11><jnl>D. Mosconi, M. Blanco, T. Gatti, L. Calvillo, M. Otyepka, A. Bakandritsos, E. Menna, S. Agnoli, G. Granozzi, *Carbon* **2019**, *143*, 318--328</jnl>.

<lit12><lit\_a><jnl>C. Su, K.<sup>^</sup>P. Loh, *Acc. Chem. Res.* **2013**, *46*, 2275--2285</jnl>; <lit\_b><jnl>D.<sup>^</sup>R. Dreyer, C.<sup>^</sup>W. Bielawski, *Chem. Sci.* **2011**, *2*, 1233--1240</jnl>; <lit\_c><jnl>D.<sup>^</sup>R. Dreyer, H.-P. Jia, C.<sup>^</sup>W. Bielawski, *Angew. Chem. Int. Ed.* **2010**, *49*, 6813--6816; *Angew. Chem.* **2010**, *122*, 6965--6968</jnl>.

<lit13><jnl>S. Presolski, M. Pumera, *Angew. Chem. Int. Ed.* **2018**, *57*, 16713--16715; *Angew. Chem.* **2018**, *130*, 16955--16957</jnl>.

<lit14><lit\_a><jnl>C.<sup>^</sup>K. Chua, M. Pumera, *Chem. Eur. J.* **2015**, *21*, 12550--12562</jnl>; <lit\_b><jnl>L. Wang, Z. Sofer, M. Pumera, *ACS Nano* **2020**, *14*, 21--25</jnl>.

<lit15><lit\_a><jnl>M. Blanco, D. Mosconi, M. Otyepka, M. Medved', A. Bakandritsos, S. Agnoli, G. Granozzi, *Chem. Sci.* **2019**, *10*, 9438--9445</jnl>; <lit\_b><jnl>J. Luo, F.

Peng, H. Yu, H. Wang, *Chem. Eng. J.* **2012**, 204--206, 98--106</jnl>; <lit\_c><jnl>B. Wang, M. Lin, T.<sup>^</sup>P. Ang, J. Chang, Y. Yang, A. Borgna, *Catal. Commun.* **2012**, 5, 96--101</jnl>; <lit\_d><jnl>Y. Kuang, H. Rokubuichi, Y. Nabae, T. Hayakawa, M.<sup>^</sup>A. Kakimoto, *Adv. Synth. Catal.* **2010**, 352, 2635--2642</jnl>.

<lit16><jnl>M.<sup>^</sup>F. Sanad, V.<sup>^</sup>S.<sup>^</sup>N. Chava, A.<sup>^</sup>E. Shalan, L. Garcia<sup>^</sup>Enriquez, T. Zheng, S. Pilla, S.<sup>^</sup>T. Sreenivasan, *ACS Appl. Mater. Interfaces* **2021**, 13, 40731--40741</jnl>.

<lit17><jnl>Y. Zhang et<sup>^</sup>al. *Chemcatchem* **2021**, doi: 10.1002/cctc.202100805</jnl>.

<lit18><lit\_a><jnl>N.<sup>^</sup>G. Sahoo, H. Bao, Y. Pan, M. Pal, M. Kakran, H.<sup>^</sup>K.<sup>^</sup>F. Cheng, L. Li, L.<sup>^</sup>P. Tan, *Chem. Commun.* **2011**, 47, 5235--5237</jnl>; <lit\_b><jnl>A.<sup>^</sup>E.<sup>^</sup>C. Collis, I.<sup>^</sup>T. Horváth, *Catal. Sci. Technol.* **2011**, 1, 912--919</jnl>.

<lit19><jnl>B. Ma, M. Blanco, L. Calvillo, L. Chen, G. Chen, T.-C. Lau, G. Dražić, J. Bonin, M. Robert, G. Granozzi, *J. Am. Chem. Soc.* **2021**, 143, 8414--8425</jnl>.

<lit20><jnl>H. Seelajaroen, A. Bakandritsos, M. Otyepka, R. Zbořil, N.<sup>^</sup>S. Sariciftci, *ACS Appl. Mater. Interfaces* **2020**, 12, 250--259</jnl>.

<lit21><jnl>B. Reuillard, M. Blanco, L. Calvillo, N. Coutard, A. Ghedjatti, P. Chenevier, S. Agnoli, M. Otyepka, G. Granozzi, V. Artero, *ACS Appl. Mater. Interfaces* **2020**, 12, 5805--5811</jnl>.

<lit22><jnl>M. Blanco, D. Mosconi, C. Tubaro, A. Biffis, D. Badocco, P. Pastore, M. Otyepka, A. Bakandritsos, Z. Liu, W. Ren, S. Agnoli, G. Granozzi, *Green Chem.* **2019**, 21, 5238--5247</jnl>.

<lit23><jnl>D. Zaoralova, R. Mach, P. Lazar, M. Mendev', M. Otyepka, *Adv. Mater. Interfaces* **2021**, 8, 2001392</jnl>.

- <lit24><lit\_a><jnl>A.<sup>^</sup>F. Carvalho, A.<sup>^</sup>J.<sup>^</sup>S. Fernandes, M.<sup>^</sup>B. Hassine, P. Ferreira, E. Fortunato, F.<sup>^</sup>M. Costa, *Appl. Mater. Res.* **2020**, *21*, 100879</jnl>; <lit\_b><jnl>C. Zhao, X. Song, Y. Liu, Y. Fu, L. Ye, N. Wang, F. Wang, L. Li, M. Mohammadniaei, M. Zhang, Q. Zhang, J. Liu, *J. Nanobiotechnol.* **2020**, *18*, 142</jnl>; <lit\_c><jnl>A. Narita, C. Chen, Q. Chen, K. Müllen, *Chem. Sci.* **2019**, *10*, 964--975</jnl>; <lit\_d><jnl>L. Wang, Z. Sofer, D. Bouša, D. Sedmidubský, Š. Huber, S. Matějková, A. Michalcová, M. Pumera, *Angew. Chem. Int. Ed.* **2016**, *55*, 13965--13969; *Angew. Chem.* **2016**, *128*, 14171--14175</jnl>; <lit\_e><jnl>N.<sup>^</sup>S. Rajput, S. Al<sup>^</sup>Zadjali, M. Gutierrez, A.<sup>^</sup>M.<sup>^</sup>K. Esawi, M. Al<sup>^</sup>Teneiji, *RSC Adv.* **2021**, *11*, 27381--27405</jnl>; <lit\_f><jnl>S. Deng, V. Berry, *Mater. Today* **2016**, *19*, 197--212</jnl>.
- <lit25><lit\_a><jnl>M. Komoda, Y. Nishina, <?><?> *Journal*<?><?> **2021**, *50*, 503--509</jnl>; <lit\_b><jnl>S. Pei, Q. Wei, K. Huang, H. C. M. Cheng, W. Ren, *Nat. Commun.* **2018**, *9*, 145</jnl>.

Commentato [gg1]: Chem. Lett.

*Matías Blanco is an organic chemistry educated at Universidad de Oviedo, Spain, where he also was awarded with the PhD degree in 2015. He has conducted his research as postdoctoral in IMDEA Nanoscience (Madrid, Spain), University of Padova (Italy) and Universidad Autónoma de Madrid (Spain) where he is currently Lecturer. His interests relay on the functionalization of nanomaterials as Carbon nanotubes, Graphene derivatives and other 2D materials for the development of catalytic hybrids with enhanced activity.*<memr1>

*Stefano Agnoli is associate professor at the University of Padova. He was awarded the Nasini medal by the Italian Chemical Society in 2015 and a Fulbright fellowship in 2017. His research interests include 2D materials and complex oxides, heterogeneous thermal- and electro- catalysis, and the development of new methods for materials characterization.*<memr2>

*Gaetano Granozzi is full professor of Solid State and Surface Chemistry at University of Padova since 1990 and is the leader of the Surface Science and Catalysis group and Editor in Chief of the journal Surfaces (MDPI). Research interests are in the areas of materials'*

chemistry, with particular emphasis on surface chemistry, heterogeneous catalysis and electrocatalysis ([www.chimica.unipd.it/surfacescience/](http://www.chimica.unipd.it/surfacescience/).<memr3>

Figure<sup>1</sup> (a) Schematic structure of graphene oxide outlining the great heterogeneity of the oxygen-based surface groups; (b) an idealized structure of graphene acid (other oxygen-based surface groups are not pictured).

Figure<sup>2</sup> The two-step synthetic procedure implemented by Bakandritsos *et al.* to introduce carboxyl groups into the basal plane of graphene.<sup>[10a]</sup> Fluorine atoms: green; Cyano groups: light blue; Carboxyl groups: red.

Figure<sup>3</sup> (a) Temporal evolution of the oxidation of benzyl alcohol to benzaldehyde and benzoic acid catalytic by GA and GO. (b) Sketch of the catalytic cycle proposed for GA.<sup>[15]</sup>

Figure<sup>4</sup> (a) Comparison of the ORR activity of N-GA, N-GA-800 (heated at 800°C) and GO. Polarization curves obtained by rotating disk electrode (solid lines) and current for H<sub>2</sub>O<sub>2</sub> production obtained by rotating ring-disk electrode (dashed lines) are reported. The role of the carboxyl functions is outlined by the comparison of the data of N-GA and N-GA-800 (the COOH groups are removed at high temperature). (b) DFT calculations results of the free-energy diagram for 2e<sup>-</sup> ORR catalyzed by N-GA.<sup>[17]</sup>

Figure<sup>5</sup> (a) Functionalization steps used to prepare GA-PDA-C-Fc and GO-PDA-C-Fc. (b) Fe 2p photoemission region of GA-PDA-C-Fc and GO-PDA-C-Fc. (c) Kinetic profiles for the C-C-H insertion reaction catalyzed by GA-PDA-C-Fc (green squares), GO-PDA-C-Fc (violet dots), molecular Fc (black triangles) and pristine GA (light green triangles).<sup>[11]</sup>

Figure<sup>6</sup> (a) Functionalization steps used to prepare Coqpy@GA. DCC= dicyclohexyl carbodiimide, HOBt= 1-hydroxybenzotriazole hydrate. (b) CO (blue) evolution in acidic conditions and formate (brown) evolution in basic conditions during CO<sub>2</sub> photochemical reduction with Coqpy@GA. Residual hydrogen evolution for both conditions is also plotted. (c) Schematic draw of the chlorine anion loss of the pristine Coqpy complex after grafting.<sup>[19]</sup>

Figure<sup>7</sup> (a) Covalent functionalization of GA with the dehydrogenase (DH) enzyme. (b) Schematic picture of the reduction of CO<sub>2</sub> to methanol catalyzed by F<sub>ate</sub>DH, F<sub>ald</sub>DH, and ADH using (i) nicotinamide adenine dinucleotide (NADH) as a sacrificial cofactor and

(ii) via a direct electron injection through a functionalized graphene support without cofactors.<sup>[20]</sup>

Figure<sup>^8</sup> (a) NiArg bioinspired electrocatalyst. (b) Immobilization of the NiArg complex on GA to provide an electrode on a gas diffusion layer (GDL).<sup>[21]</sup>

Figure<sup>^9</sup> (a) Preparation of Pd nanoparticles on GA. (b) Transmission Electron Microscopy (TEM) image of GA-C-Pd-100 sample (in the inset the size histogram is reported).<sup>[22]</sup>

Figure<sup>^10</sup> (a) SM cross coupling reaction of boronic acids and organic halides. (b) Kinetic profiles of the SM reaction with different GA-C-Pd and GO-C-Pd catalysts.<sup>[22]</sup>

Figure<sup>^11</sup> (a) Preparation of Sm<sub>2</sub>O<sub>3</sub>/GA. (b) Glucose oxidation on Sm<sub>2</sub>O<sub>3</sub>/GA. (c) Catalytic cycle for glucose oxidation on Sm<sub>2</sub>O<sub>3</sub>/GA.<sup>[16]</sup>

Figure<sup>^12</sup> Electrochemical sensing of glucose by Sm<sub>2</sub>O<sub>3</sub>/GA.<sup>[16]</sup>

Scheme<sup>^1</sup> Second generation graphenes.

**Commentato [gg2]:** Be careful : in gthe pdf version oft he proofs the subscripts in the formulas are not present !!!